

Analysis of Phase Relationship in ECoG using Hilbert Transform and Information Theoretic Measures

Jeffery Jonathan (Joshua) Davis^(1,2)

¹Center for Large-Scale Optimization & Networks (CLION)
University of Memphis, Memphis TN 38152 USA

²Embassy of Peace, Whitianga New Zealand

Robert Kozma

Center for Large-Scale Optimization & Networks (CLION)
Dept. of Mathematical Sciences, University of Memphis
Memphis TN 38152 USA

Abstract—We apply Hilbert transforms to the analysis of phase relationship in electrocorticogram (ECoG) signals in order to explore a set of meaningful information theoretic measures. This analysis leads to a methodology to derive meaning from experimentally observed brain dynamics under various states induced by sensory stimuli. We explore the possibility to represent periods of habituation and learning based on instantaneous frequency signals and introducing a new set of parameters, based on the concept of pragmatic information.

Keywords:- Electroocorticogram (ECoG); Hilbert Transform; Instantaneous Phase; Instantaneous Frequency; Pragmatic Information; Shannon Entropy; Synchronization; Desynchronization; Phase Transition.

I. INTRODUCTION

In order to derive meaningful information related to the output of EEG signals based on the input of diverse kind stimuli, we require a methodology capable of processing complex signals that are highly dynamic and non linear in nature. In recent years many scientists have been exploring ways towards this goal and have gained insight and developed an initial methodology to accomplish such a difficult analysis [1-6]. In this study we continue exploring more ways of improving such a methodology. These efforts aim toward establishing a comprehensive approach to be applied to brain dynamics in a wide range of practical field, to enhance human capabilities, to provide support for the disabled, and lead to improved well-being and peaceful living in our society [7-8].

The work presented here is closely related to previous studies on nonlinear spatio-temporal dynamics of rabbit brain dynamics conducted at Dr. W.J. Freeman's Lab at UC Berkeley [2, 9]. We start with the description of the rabbit ECoG data, which concern the visual cortex, and outline the employed preliminary processing and conditioning approaches. Then we introduce the computational tools and algorithms for data evaluation. We demonstrate that our tools

reproduce previous results. As a next step, we systematically explore various frequency bands, including delta, theta, alpha, and beta bands. For the purpose of this paper we especially expand on results obtained over theta band. Next we discuss the relevance of results of the analysis for the cognitive activity, learning and habituation effects in rabbit brains. Finally, we introduce a set of ratios based on the concept of "Pragmatic Information", as an alternative and complement to the Shannon entropy index. We demonstrate the benefit of the new indices in the analysis and detection of phase transitions and de-synchronization windows in time domain. In conclusion, we comment on other studies applying the concept of Pragmatic Information. We outline the benefit of our results to build a robust comprehensive methodology to understand brain dynamics.

II. DESCRIPTION AND PREPROCESSING OF RABBIT ECOG SIGNALS

The electrical activity of the primary visual cortex in rabbits was measured using an 8*8 array of clinically implanted electrodes [9]. The space between the electrodes is 0.79 mm covering an area of 5.6mm*5.6mm. During data recording, the signals were low-pass filtered at 100 Hz. Experiments have been conducted for duration of 6 s, which have been divided into 3 s pre-stimulus and 3 s post-stimulus periods, respectively. The sampling frequency was 500 Hz, which gave a total of 3000 sample points for each of the 64 channels. The rabbits were trained to discriminate visual conditioned stimuli eliciting conditioned responses, which have been analyzed during the 3 s post-stimulus time segment.

To start our analysis, we used FIR band pass filters to obtain the signals for each band. Using Hilbert transformation, we calculated the analytic signal with analytic amplitude (AA) and analytic phase (AP). Instantaneous phase and frequency has been calculated using first-order time differentials [10-11]. From the 64 channels collected from rabbits, two channels were defective; namely # 29 and #38. Two alternatives were explored to correct this situation. One was to interpolate between immediate neighbor channels to produce an estimate

This work has been supported in part by the University of Memphis Research Foundation, through the FedEx Institute of Technology, and by a grant of the First Tennessee Fund.

of the missing signals. The other approach was to find an average of the neighbor channels in the same row. For example, channel 38 is obtained as the Mean of channels (6, 14, 22, 30, 46, 54, 62). Both methods gave almost identical results and the decision was made for method number one (interpolation between immediate neighbor channels).

We intended to use the same data as in [2, 11], however, we observed some differences when analyzing them in our work. For example, the moments of de-synchronization differ slightly from those shown in [2]. The above differences could be attributed to the filters applied to extract the signal for each band. However it seems more likely that the cause is due to a different batch of sample data.

III. RESULTS OBTAINED BY HILBERT SPACE ANALYSIS

We developed a suite of Matlab routines for data analysis. Using these routines for analyzing Hilbert transform, we evaluated the behavior for each of the four bands: Beta (16.5Hz, 21Hz), Alpha (9Hz, 11Hz), Theta (4Hz, 6Hz), and Delta (2.7Hz, 3.4Hz). In the present paper, we mention results over all these bands, but we focus on theta band. Figures 1 and 2 show results of the initial analysis of 64 channels of rabbit ECoG data over theta band: $F_{stop1}=3\text{Hz}$, $F_{pass1}=4\text{Hz}$, $F_{pass2}=6\text{Hz}$, $F_{stop2}=7\text{Hz}$. Figure 1 shows signals of all 64 channels (top), the analytic phase of the signals after Hilbert transform (middle), and absolute analytic frequency derived from the instantaneous phase differences (bottom). Figure depicts unwrapped instantaneous phases (top), instantaneous frequency (middle), and the histogram of the instantaneous frequency for 64 channels in the theta band.

We observe that the channels move together most of the time, thus highly synchronized. However, there are moments of desynchronization with significant dispersion of the signal amplitudes and phases. The analytic frequency is especially suited to characterize the changes. Namely, there are spikes in the analytic frequency at time instants 1.2s, 2.8s, 3.1s, and so on, indicating sudden changes in the analytic signal behavior. Exactly these are the periods when the synchronization between channels apparently breaks down. We also generated movies to illustrate the desynchronization events, which are available upon request.

We observe similar synchronization-desynchronization behavior over all frequency bands; which are not shown here due to the limited space. The four bands present different windows of de-synchronization events where some visual approximations have been made based on the graphs in Fig. 1. Next we point out which time instances demarcate the de-synchronization events between 0.5s and 5.5s. Visual inspection of the plots over time indicates that these desynchronization events were related to overall changes in amplitude during these periods.

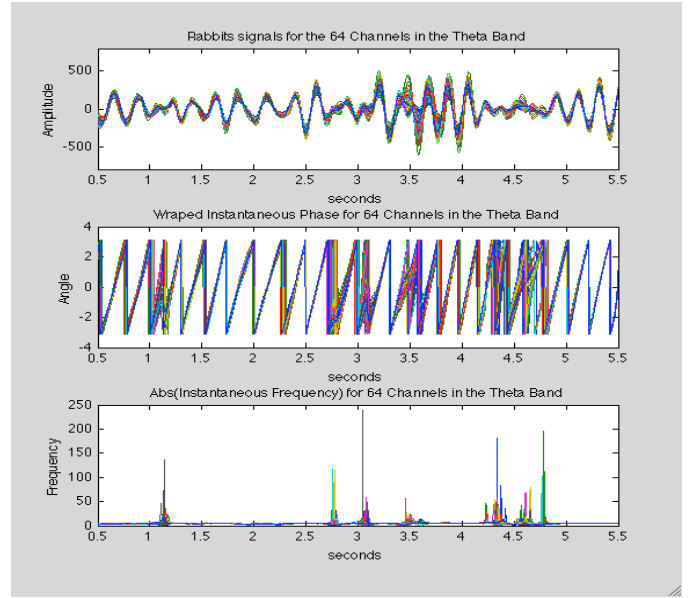


Figure 1. Illustration of the analyzed rabbit ECoG data filtered over theta band; ($F_{stop1}=3\text{Hz}$, $F_{pass1}=4\text{Hz}$, $F_{pass2}=6\text{Hz}$, $F_{stop2}=7\text{Hz}$); top: signals of all 64 channels; middle: analytic phase of the signals after Hilbert transform; bottom: absolute analytic frequency derived from the instantaneous phase differences.

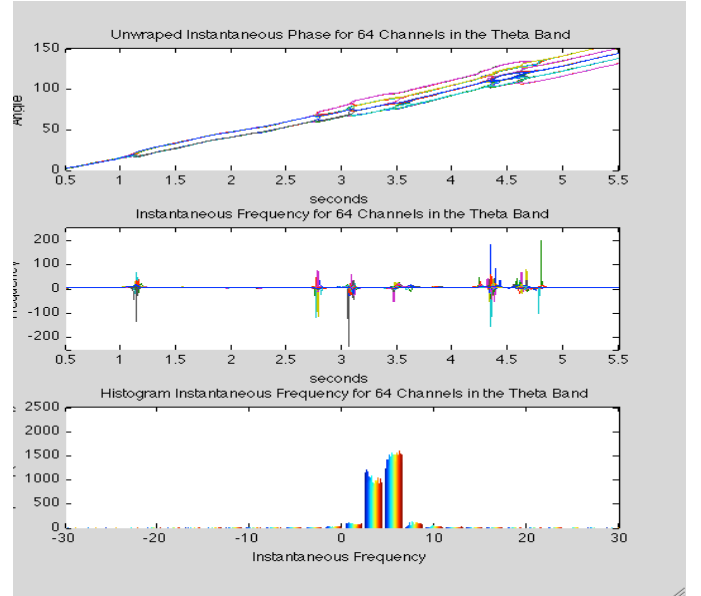


Figure 2. Phase relationships of the analytic signal of the rabbit ECoG channels over the theta band; top: unwrapped phase for all 64 channels; middle: analytic frequencies; bottom: histogram of instantaneous frequencies.

Table I summarizes the observed de-synchronization events between channels and the corresponding behavior in the amplitude. An arrow that is pointing up (\uparrow) is used to describe increased amplitude, while an arrow pointing down (\downarrow) describes decreased amplitude. We observe that there is significantly more activity in the Beta band than everywhere else. Delta shows the lowest activity while, Theta and Alpha show a little bit more activity than Delta. All bands show de-synchronization activity around 3.5s with increased amplitude.

Table I Summary of the observed de-synchronization windows over all 4 frequency bands

Delta Band	
Time Event	1.1 1.5
Amplitude	↓ ↓
Theta Band	
Time Event	1.1 2.8 3.1 3.5 4.3 4.6 4.8
Amplitude	↓ ↓ ↑ ↑ ↓ ↓ ↑
Alpha Band	
Time Event	0.6 2.0 2.4 3.6 3.7 4.5 4.7 5.3
Amplitude	↓ ↓ ↓ ↓ ↑ ↑ ↓ ↓ ↑
Beta Band	
Time Event	0.6 0.8 1.3 1.5 1.7 1.8 2.1 2.2 2.4 2.5 2.6 2.7 3.0 3.2 3.5 3.7 4.1 4.4 4.5 4.7 4.9 5.3 5.4
Amplitude	↓ ↓ ↓ ↓ ↓ ↑ ↑ ↓ ↓ ↓ ↓ ↓ ↓ ↓ ↓ ↑ ↑ ↓ ↓ ↓ ↓ ↑

Most of the observed amplitude behaviors match for all bands in de-synchronization windows. The exceptions are time point 3.8 s for the Delta band, and 4.8 s for the Theta band, which appear by themselves. Note that the Alpha and Beta bands are the first ones to show de-synchronization as well as activity after 5 s. In the interval 4.5 to 4.6 s, Alpha, Beta and Theta show de-synchronization and the amplitude drops for all of them. It is important to note that for each moment of de-synchronization there seems to be a general or average drop in Amplitude; see Fig. 3.

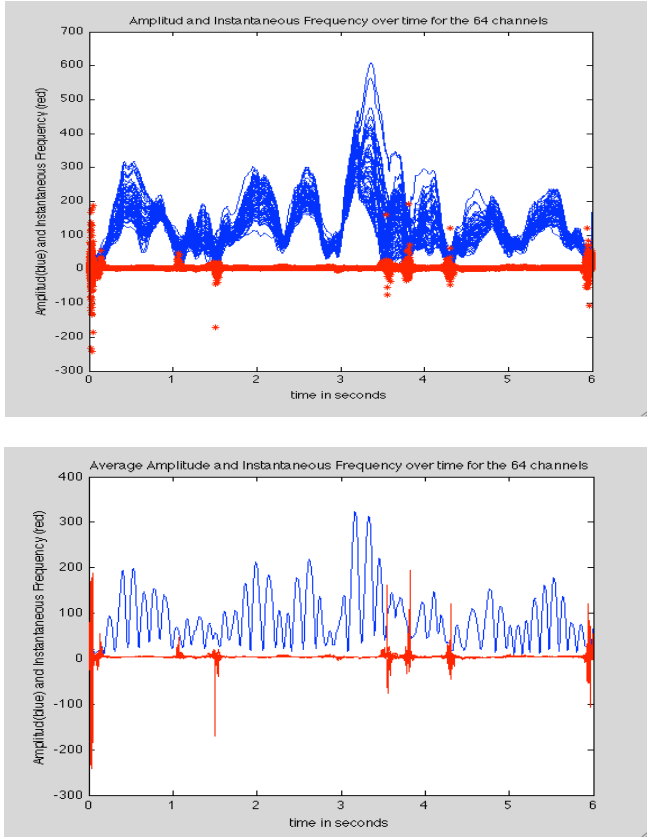


Figure 3. Illustration of the correlation between drop in analytic amplitude (blue) and spike in instantaneous frequency (red); top: all 64 channels; bottom: spatial ensemble average of 64 channels.

In general, the Amplitude range of the signal is higher when the system is in phase synchronization mode, while the amplitude range of the signal is lower in periods of phase de-synchronization. Also we observe that between the periods 3.4-3.8 s, the amplitude range of the signal is the highest. It seems necessary to explore this period more deeply with some contrasting ratios relating analytic amplitude and phase.

The events occurring before the 3s and after 4s seem to have a different influence on the amplitude than the events occurring between the 3.5s-3.8s window. In that time window, the amplitudes in some channels go up and in some others go down, instead of all moving in the same direction. We observe that this is the period for which the amplitude range of the signal is the highest. This is also observed for the Analytical Amplitudes (AA). This specific window corresponds with the post-stimulus period when the rabbit's cognitive activity is the highest following the conditioned learning. Thus it may be hypothesized that the observed effect is related to learning, when a "New Behavioral Habituation Map" competes/ intervenes with the "Old Behavioral Map."

Further detailed studies are needed to determine the interdependence between bands in relation to the learning task, tolerance, assimilation of learning, learning delays, and habituation. Possible indication of such effect may be observed particularly in situations like the one observed between 3.5-3.6 s, where all bands show de-synchronization activity. This can be regarded as an *overall synchronization of the desynchronization across all bands*, while most desynchronization effects are limited to a few bands, or to a specific frequency band [12].

IV. INFORMATION-THEORETIC INDICES AND RATIOS

In this section we develop a qualitative characterization of the empirically observed synchronization-desynchronization effect described previously. We are introducing several indices and ratios based on the Amplitudes (Both Analytical Amplitude and Original Signal's Amplitude) for a fixed window that moves across the axis of time. These indices are based on [7, 10], but introduce some novel aspects as well.

These indexes and ratios are plotted both for each group channel and for the average for each group channel (group1=1:8, group2=9:16,..., group7=49:56). Following are the indexes relevant to our analysis:

- *Range (max-min)* of Amplitude for each channel, (ra_i). The Amplitude can be the signal amplitude, analytic amplitude, or squared analytic amplitude.
- *Euclidean Distance* (ED or ED_{group}). This is calculated in the present study based on the instantaneous phase between contiguous channels, ($ed_{i,i+1}$ for $i=1,63$),
- *Shannon Entropy Index* (SH) for each channel, (sh_i) This index is computed with Matlab entropy index routine.

Any specific Index (I) is calculated in the general form:

$$I = \text{Mean}(\text{Amplitude}) / \text{Mean}(\text{ED}) \quad (1)$$

Here *Amplitude* can be one of the following RSA, RAA, or MA2 as defined below:

- *RSA*: The Range of the signal's Amplitude for a fixed window of time
- *RAA*: The Range of the Analytical Amplitude for a fixed window of time
- *MA2*: The Squared Mean of the Analytical Amplitude for a fixed window of time.

After these preliminary definitions, we are ready to introduce the Pragmatic Information Index, following Freeman's work [4, 13-14]. However, we experiment with alternative definitions and introduce 3 variants to the Pragmatic Information Index. The following Pragmatic Information Indices are studied in this work:

$$IRSA = RSA/ED, \quad (2)$$

$$IRAA = RAA/ED, \quad (3)$$

$$IMA2 = MA2/ED. \quad (4)$$

Figure 4 shows the Pragmatic Information Index IMA2 calculated using Eq. 4 for the squared mean of the analytic amplitude (AA) over 50 consecutive time segments in the interval 0.5s to 5.5s. The applied frequency band is theta (4Hz to 6Hz). The top figure shows the group indices for the 7 groups of instantaneous phases as defined by the Euclidean Distance (ED); the bottom figure illustrates the ensemble average index over the whole array. Clearly, the index has periods of significant increase and consequent drop over the studied time window.

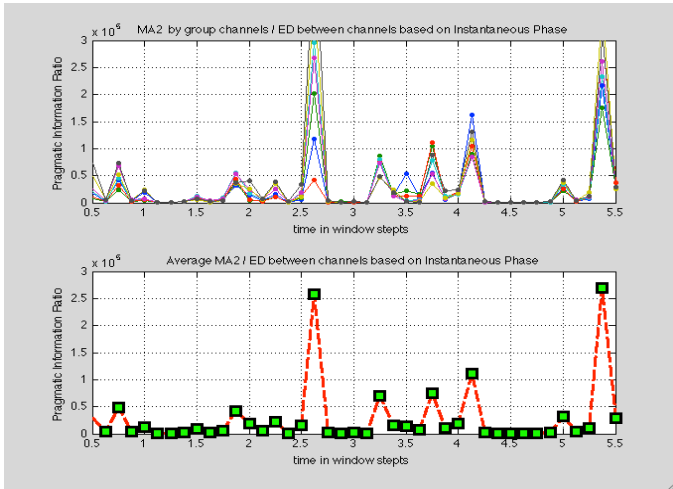


Figure 4. Pragmatic Information Index IMA2 calculated using the squared mean of analytic amplitudes over the theta band; top: group indices for the 7 groups of instantaneous phases as defined by the Euclidean Distance (ED); bottom : ensemble average index over the whole array.

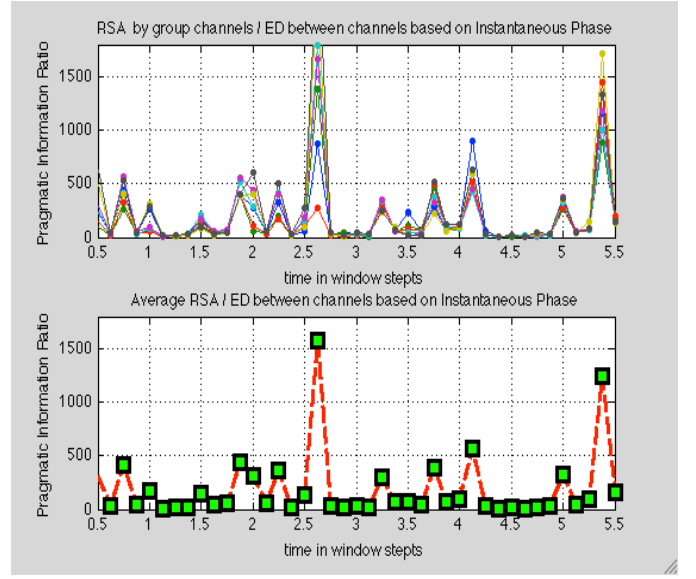


Figure 5. Pragmatic Information Index IRSA calculated using the range of the original signal amplitudes over the theta band; top: group indices for the 7 groups of instantaneous phases as defined by the Euclidean Distance (ED); bottom : ensemble average index over the whole array.

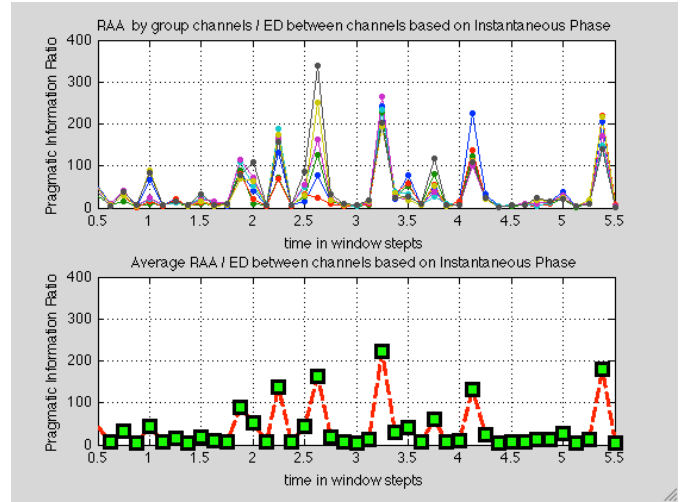
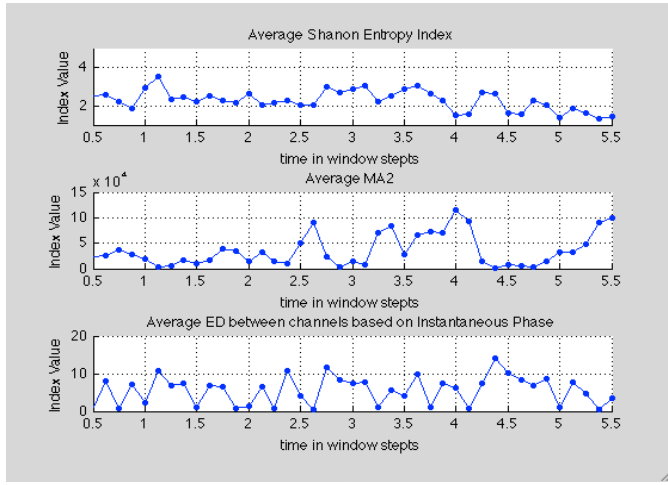
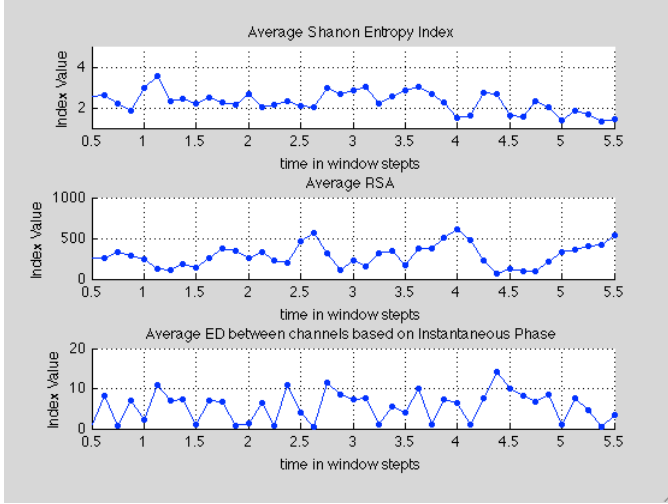


Figure 6. Pragmatic Information Index IRAA calculated using the mean of the range of analytic amplitudes over the theta band; top: group indices for the 7 groups of instantaneous phases as defined by the Euclidean Distance (ED); bottom : ensemble average index over the whole array.

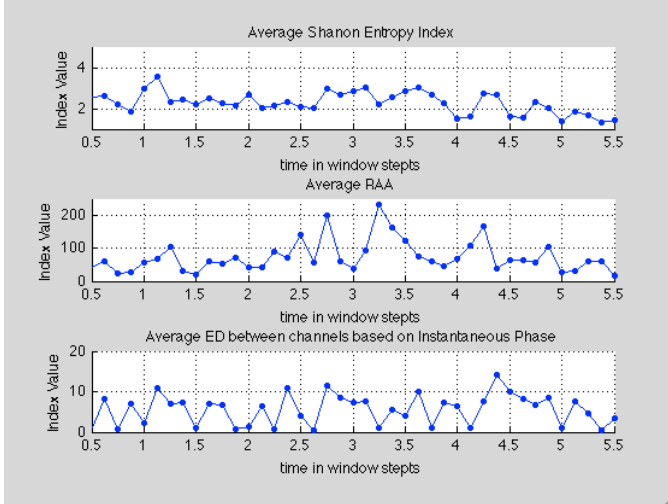
Figure 5 shows the Pragmatic Information Index IRSA calculated using Eq. 2 for the mean of the signal amplitudes over the theta band; notations are similar to Fig. 4. Finally, Fig. 6 shows the IRAA index based on the mean range of analytic amplitudes (AA) over theta band. All the indices exhibit spikes at given time instances. These spikes have some common features across index types, but they are not identical. Clearly, they reflect various aspects of the underlying brain dynamic process. In order to understand the behavior of these indices, in Fig. 7 and 8 we depict the components of these indices, namely the various Amplitude range measures, the Euclidean Distances, as well as the Shannon index.



(a)

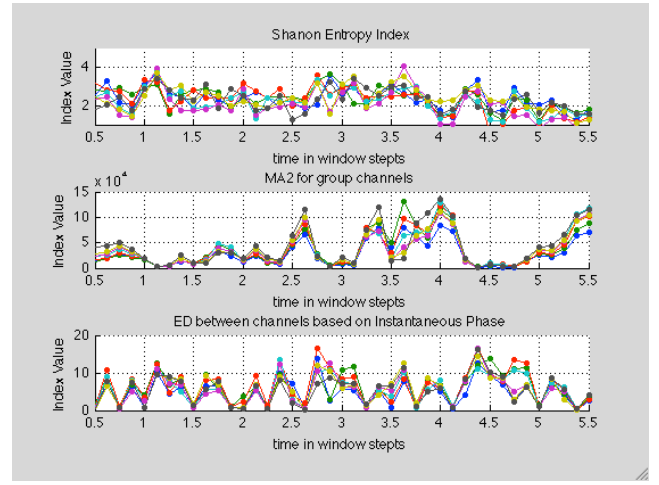


(b)

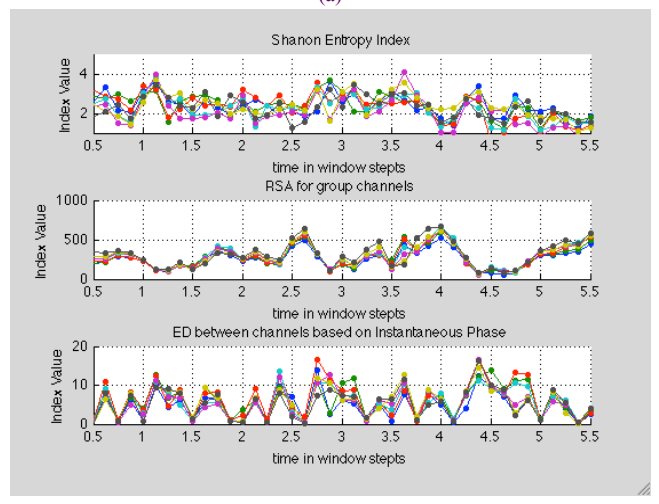


(c)

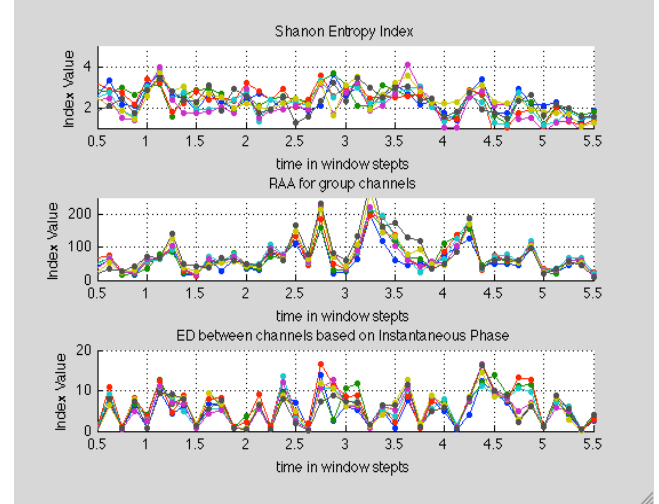
Figure 7. Average indices across the array: Shannon Entropy Index (top), Amplitude measures (middle), and Euclidean Distance (bottom) calculated over 50 time steps; (a) case of mean squared analytic amplitude (MA2); (b) Range of signal amplitude (RSA); (c) Range of analytic amplitude (RAA).



(a)



(b)



(c)

Figure 8. Segment-wise indices for groups of channels: Shannon Entropy Index (top), Amplitude measures (middle), and Euclidean Distance (bottom) calculated over 50 time steps; (a) case of mean squared analytic amplitude (MA2); (b) Range of signal amplitude (RSA); (c) Range of analytic amplitude (RAA).

V. DISCUSSIONS

Our results confirm, as a general rule, that the analytic amplitude (AA) drops for time instances when the phase breaks happen. This is the manifestation of the behavior what Freeman calls null spike [4]. However, in the time window of about 1s after the stimulus, we observe a more complicated behavior. We observe for AA that in the window mentioned before, and especially at 3.5s-3.8s, some channels shoot up while the rest of them (majority) are dropping. This happens for all the channels studied and seems to be more prominent on the theta and delta bands. In addition, we observe between 3s - 3.75s that the great majority of ED levels are high, meaning again a significant high phase break.

Detailed analysis indicates that a very interesting event is happening between 3.375s and 3.5s. Here the ED still shows significant phase break, and all the amplitude indexes move in the same direction as ED. It is exactly in this situation where we find the kind of meta-stability between the two competing-tendencies occur, i.e., habitual patterns and learning. This is shown in the graphs for all amplitude measures RSA, RAA and MA2. Some of the channels are going up and some down when the system is willing to synchronize for a moment while de-synchronization takes over. Note that ED at this point may represent medium de-synchronization level, where the system may be both synchronizing and desynchronizing at the same time. It is important to say that all other windows with Significant Phase Break show constant levels for the IRSA and MA2 ratios in contrast with the windows mentioned above (3.375s and 3.5s). This further reinforces our interest in this window with very unique dynamic properties.

Generally speaking, moments of greater values for ED show greater values for SH, something we would expect. When SH is contrasted with ED in the theta band, we observe that they both follow a similar trend, something that matches our expectation that the stronger the Phase Break measured by ED, then the highest the entropy we should observe in SH. Note that we used the Shannon Entropy Index (SH) provided by Matlab as a measurement to be contrasted with ED. Furthermore, it is expected to be beneficial to consider all the possible variations between channels to calculate the ED based on the difference of the instantaneous phase between two channels and their characteristics. We should explore ED as the average of all possible combinations ($64 \times 63/2 = 2016$) as a substitute index for the one we have used ($ED_k = \text{Average}(ed_{i,j+1} \text{ for } i=1,63)$) for each group $k=1:7$. We have left group 8 out of this analysis because it would only have 7 members instead of 8. However in the future we could include this group even in the face of this limitation to explore and have a sense of how this group is behaving. We could also test statistically the significance of the sample size for this group to make sure it is appropriate to include it. Also we could solve this situation by using the Average (ED) for the 2016 possible combinations and include group channel 8 (57:64).

The theta band seems to be quite unique in the sense of its rich spatio-temporal dynamics as manifested in ECoG recordings. This indicates the need for further attention to better appreciate some distinctions with other bands as portrayed in the IRSA for the window 3s to 3.75s. The de-synchronization events can be appreciated more dramatically for all windows in the peaks and drops (almost like cycles). However, that could just be a matter of scale when we look closer in other ratios across different bands.

VI. CONCLUSIONS AND FUTURE PERSPECTIVES

The present work contains results of the analysis of ECoG experimental data with a range of information-theoretic indices and ratios in order to extract cognitively relevant content from array recordings.

Preliminary analysis indicates that there are a lot of time windows where the (RSA, RAA, MA2) indexes present an opposite direction to ED. Another typical behavior is shown by windows where the (RSA, RAA, MA2) indexes present the same direction to ED. Consequently, the ratio between them (RSA/ED, for example) would behave differently in different situations, something difficult to predict depending of which index (RSA or ED) grows more proportional to each other. So far this is a preliminary analysis and it is recommended that it would be done for all bands.

These indexes only gave us a partial idea of what is going on and other approaches are also justified and indeed required to better explain brain dynamics and its correlates to cognitive functions and consciousness. Many-body field dynamics, for example, is a very promising approach and can provide valuable motivation to experimental analysis and modeling [15].

The present work is focused on theta band, but clearly various bands have rich behaviors which should be thoroughly investigated. Preliminary results indicate that the different indexes (MA2, RSA, RAA) seem to display a similar trend between bands only for the RAA index apart from theta. We expect to gain significant new insights by simultaneously analyzing these bands and their interference.

ACKNOWLEDGMENT

Experimental data on rabbit ECoG are the courtesy of Prof. Walter J. Freeman's Neurophysiology Laboratory, Division of Neurobiology, UC Berkeley, which is greatly appreciated. J.D. is indebted to the supportive environment at the Embassy of Peace, Whitianga, NZ, making the completion of this study possible.

REFERENCES

- [1] Freeman WJ [2008] A pseudo-equilibrium thermodynamic model of information processing in nonlinear brain dynamics. *Neural Networks* 21: 257-265.
- [2] Kozma, R., Freeman, W.J. (2008) Intermittent spatio-temporal desynchronization and sequenced synchrony in ECoG signals, *Chaos*, 18, 037131.

- [3] Logothetis NK (2008) What we can do and what we cannot do with fMRI. *Nature* 453: 869-878. doi:10.1038/nature06976
- [4] Freeman WJ (2009) Deep analysis of perception through dynamic structures that emerge in cortical activity from self-regulated noise. *Cog Neurodyn* 3(1): 105-116.
- [5] Ruiz Y, Pockett S, Freeman WJ, Gonzales E, Li Guang (2010) A method to study global spatial patterns related to sensory perception in scalp EEG. *J Neuroscience Methods* 191: 110-118. doi:10.1016/j.jneumeth.2010.05.021
- [6] Freeman WJ, Livi R, Opinata M, Vitiello G (2012) Cortical phase transitions, non-equilibrium thermodynamics and the time-dependent Ginzburg-Landau equation. *Int J Mod Phys B* (in press) arxiv:1110.3677v1 [physics.bio-ph]
- [7] Jeffery Jonathan (Joshua) Davis (2009) *The Brain of Melchizedek, Thesis*, Otago University, Dunedin, New Zealand.
- [8] Freeman WJ (2011) Understanding perception through neural 'codes'. In: Special Issue on "Grand Challenges in Neuroengineering", *IEEE Trans Biomed Engng.* 58 (7): 1884-1890. DOI: 10.1109/TBME.2010.2095854
- [9] Barrie JM, Freeman WJ, Lenhart M (1996) Modulation by discriminative training of spatial patterns of gamma EEG amplitude and phase in neocortex of rabbits. *J Neurophysiol* 76:520-539
- [10] Freeman WJ (2007) The Hilbert transform for EEG. *Scholarpedia* 2(1): 1338. <http://repositories.cdlib.org/postprints/2781>
http://www.scholarpedia.org/article/Hilbert_transform_for_brain_waves
- [11] Rodriguez, J.M., Kozma, R. (2007) Phase synchronization in mesoscopic encephalogram arrays. *Proc. ANNIE2007, Vol. 17, pp. 3-8*, ASME Press.
- [12] Bullock T.H., McClune M.C., Achimowicz J.Z., Iragui-Madoz V. J., Duckrow R. B., and Spencer S.S. (1995) Temporal fluctuations in coherence of brain waves, *Proc. Natl. Acad. Sci. USA* Vol. 92, pp. 11568-11572.
- [13] Freeman W.J. (2005) "Origin, structure, and role of background EEG activity. Part 3. Neural frame classification". *Clin. Neurophysiol.*, 116 (5): 1118-1129. <http://escholarship.org/uc/item/8z1201cb>
- [14] Freeman WJ, Vitiello G (2006) "Nonlinear brain dynamics as macroscopic manifestation of underlying many-body field dynamics". *Phys Life Rev* 3: 93-118. <http://dx.doi.org/10.1016/j.plev.2006.02.001>.
- [15] Freeman W.J. *Mesoscopic Brain Dynamics*. (2000) Great Britain, Springer – Verlag, London Limited.